Development of Solid Lipid Nanoparticles and Nanostructured Lipid Carriers of Loteprednol Etabonate: Physicochemical Characterization and Ex Vivo Permeation Studies

Burcu Üner (uner.burcu@yahoo.com)
Istanbul University: Istanbul Universitesi https://orcid.org/0000-0003-4691-0432
Samet Özdemir
Istanbul Health and Technology University: Istanbul Saglik ve Teknoloji Universitesi
Çetin Taş
Yeditepe University: Yeditepe Universitesi
Yıldız Özsoy
Istanbul University: Istanbul Universitesi
Melike Üner
Istanbul University: Istanbul Universitesi

Research Article

Keywords: Loteprednol etabonate, nanostructured lipid carriers, solid lipid nanoparticles, topical corticosteroids, transdermal delivery

Posted Date: December 10th, 2021

DOI: https://doi.org/10.21203/rs.3.rs-1145116/v1

Abstract

Purpose Loteprednol etabonate (LE) is a new generation corticosteroid that is used for the treatment of inflammatory and allergic conditions of the eye, and management of seasonal allergic rhinitis nasally. LE which is a poorly soluble drug with insufficient bioavailability, has a high binding affinity to steroid receptors. Sophisticated colloidal drug delivery systems of LE could present an alternative for treatment of inflammatory and allergic conditions of the skin. For this purpose, solid lipid nanoparticles (SLN) and nanostructured lipid carriers (NLC) were attempted to improve for transdermal LE delivery for the first time.

Methods SLN and NLC were produced by hot homogenization and ultrasonication technique. Formulations were characterized by dynamic light scattering, scanning electron microscopy, fourier transform infrared spectroscopy and differential scanning calorimetry. Their physical stability was monitored for 3 months of storage. Drug release profiles and permeation properties of SLN and NLC through the porcine skin were investigated.

Results It was determined that SLN and NLC below 150 nm particle size had a homogeneous particle size distribution as well as high drug loading capacities. They were found to be stable both physically and chemically at room temperature for 90 days. In terms of release kinetics, it was determined that they released from SLN and NLC in accordance with Fickian diffusion release. Formulations prepared in this study were seen to significantly increase drug penetration through pig skin compared to the control group ($p \leq 0.05$).

Conclusion SLN and NLC formulations of LE can be stated among the systems that can be an alternative to conventional systems with less side-effect profile in the treatment of inflammatory problems on the skin.

Introduction

Treatment of skin diseases includes various medications. Topical corticosteroids have been used and provided an effective therapy. Moreover, they are employed to provide anti-inflammatory, antimitotic, and immunosuppressive actions (1). These pharmacological actions depend on various mechanisms. The utilization of topical corticosteroids for specific skin diseases is discussed in detail in the relevant review studies (2, 3). The use and adverse effects of intralesional and systemic corticosteroids are discussed separately. Loteprednol etabonate (LE) is a topical corticosteroid that was synthesized via modification of prednisolone to achieve the desired anti-inflammatory action followed by rapid conversion to inactive metabolites (4, 5). Data from pharmacokinetic studies of LE indicate that it undergoes a high first-pass effect in the liver, is rapidly eliminated from the systemic circulation. Its plasma half-life is 2.8 h and is highly bound to plasma proteins (6). In addition, studies are showing that LE is more lipophilic (log k = 3.04) and has a low water solubility (0.5 µg/mL) compared to commonly used corticosteroids such as hydrocortisone and dexamethasone (7).

Semi-solid dosage forms such as ointments, creams or gels are used for the treatment of skin diseases. The drug penetration through the skin is low and possesses high variation (8). Innovative systems consisting of carrier systems with nanometer size can be an alternative to overcome various problems encountered in transdermal penetration. Nanocarrier systems have become one of the areas where researchers frequently work, especially since they are used specifically for the region where both diagnostic and therapeutic agents will be loaded and the drug will be effective in a controlled and targeted way (9) These colloidal systems (lipid nanoparticles, liposomes, and micro/nanoemulsions) are becoming the focus of attention due to their passage through the stratum corneum, which is the upper layer of the skin, and increasing uptake in the stratum corneum (10). These nanostructured systems are generally 2 or more layered carrier systems consisting of lipids and other components such as surfactants in high proportion (liposomes, etosomes, transferosomes, niosomes, phytosomes e.t.c.) (11, 12). Short shelf life, low stability and encapsulation efficiency, rapid elimination from circulation by immune system cells, and interaction with various cells are the major disadvantages of these systems (13).

Solid lipid nanoparticles (SLN) and nanostructured lipid carriers (NLC) have been developed as alternatives to carrier systems such as liposomes, niosomes and transferosomes, due to their non-artificial components and their low cost (14).These lipid colloid systems have sizes from 40 nm to 1000 nm. In addition, they consist of solid/liquid lipids and surfactants, which are considered safe materials. They have many advantages such as allowing large-scale production, high chemical and physical stability, and enabling targeted therapy (14, 15). In SLN, the liquid lipid found in conventional emulsion formulations has been replaced by solid lipids in glycerides or waxes. Therefore, SLNs maintain the release of the active substances they contain for a long time due to the depot effect. NLC, also known as new generation lipid nanoparticles, emerged as a result of the use of liquid and solid lipids together. SLN and NLC increase the penetration and indirectly the permeation of the drug by clogging the skin (occlusive effect) so that the skin does not lose its moisture and therefore provides skin hydration. While increasing permeation due to this process, they also provide a controlled drug release thanks to their depot effects. Since they consist of non-toxic and non-irritable lipids, they can be used easily on inflammation and damaged skin (17).

A new formulation design is required to overcome such high lipophilicity, the low solubility of LE, and the high side-effect profile. In this study LE loaded SLN and NLC were prepared and characterized, respectively. Then, in vitro and ex vivo, drug release studies were performed to determine the release profile of the SLN and NLC.

Only traditional eye drops and nasal sprays of LE are available in the pharmaceutical market. There is no previous study on the skin application of this substance which has a higher binding affinity to steroid receptors compared to dexamethasone. Sophisticated colloidal drug delivery systems of LE could present an alternative for treatment of inflammatory and allergic conditions of the skin. SLN and NLC of LE were attempted to be designed for its transdermal delivery for the first time. For this purpose, SLN and NLC were produced by hot homogenization and ultrasonication technique. They were characterized by

morphological screening, particle size and zeta potential measurements, and investigation of drug:excipient interaction and thermal behaviours of solid lipids in nanoparticles. In vitro drug release properties of the formulations and the permeation of LE through full-thickness porcine skin were investigated. was studied.

Materials And Methods

Materials

Loteprednol etabonate (LE) was gratefully donated by Deva İlaç Sanayi ve Tic. A.Ş. (Turkey). Compritol® 888 ATO, Compritol® E ATO, and 1-tetradecanol were kindly provided by Gattefossé (France). Cutina® CP, Geleol™, Gelucire® 50/13, Imwitor® 491, Imwitor® 900K, Isopropyl myristate, and cetostearyl alcohol were purchased from Ataman Kimya A.Ş. (Turkey). Oleic acid and castor oil were purchased from BASF (Germany). Olive oil purchased from Arpaş Arifoğlu Pazarlama Dağıtım ve Ticaret A.Ş. (Turkey). Cremephor® EL, cetostearyl alcohol (CA), Nacol 16-98, and Cremephor® RH40 were provided from Sigma-Aldrich (Germany). Lutrol® F68, Tween® 80, and Labrasol® were purchased from BASF (USA). All other chemicals were of analytical grade.

Methods

Screening of Lipid and Oil

The solubility of LE in several solid and liquid lipids was determined by adding a specific amount of LE in 500 mg of the lipids separately in vials. The vials containing drug and solid lipid mixtures were then stored at 80 ± 5.0°C (19). 1-tetradecanol, cetyl alcohol, cetyl palmitate, CA, Compritol® E ATO, Compritol® 888 ATO, Cutina® CP, Geleol™, Gelucire® 50/13, Imwitor® 491, Imwitor® 900K, Nacol® 16-98, Softisan® 141, Softisan® 601, and stearic acid were used as solid lipids for this purpose. At the same time, the solubility of LE in 500 mg of the liquid lipids (isopropyl myristate, oleic acid, castor oil, and olive oil) separately in 5mL sealed vials and they were stored at 80 ± 5.0°C. The vials were taken and centrifuged at 3000 rpm for 30 min. The clear supernatant was isolated and filtered (0.22 µm filter was used). The concentration of LE was determined by using a high performance liquid chromatography (HPLC) method (20).

The solubility of LE in a group of surfactants (Cremophor® EL, Cremophor® RH 40, Lutrol® F68, Tween® 80 and Labrasol®) was also achieved by using the method specified for screening of oils (19). The vials were placed at 80 ± 5.0°C. The samples were taken and centrifuged at 3000 rpm for 30 min. The clear supernatant was isolated and filtered. The amount was calculated by using the HPLC method. After the surfactant imaging study, classical emulsions were prepared at 80 ± 5.0°C and the emulsions were examined in terms of phase separation and fluidity (19).

Solubility Study

The solubility of LE was studied both in water and phosphate buffered saline (PBS) at pH 7.4. 10 mL solutions were placed in four flasks (the volume of each flask was 20 mL). The greater quantity of the drug was added to each flask to provide saturation of the solution. Flasks containing a mixture in equilibrium with solid were tightly closed. Then, they were placed in an orbital shaker (bioSAN, S20-60, Riga, Latvia) at room temperature. Apparatus was adjusted to 150 rpm shaking rate for 24 h. Dispersions were filtered by using a membrane filter (0.45 µm). A portion of supernatants was taken from flasks. The solubility of LE in the filtrate was analyzed at 273 nm (Agilent 8453 UV-spectrophotometer, USA) (21).

Measurement of LE amount and Analytical Method Validation

The quantity of LE was measured by using an HPLC method. For this goal, a previously published analytical method was developed with slight modifications, then validated (20). Briefly, an HPLC instrument (Agilent 1110, USA) equipped with a diode array detector (Agilent Tech, USA) was chosen. Stationary phase was an octadecylsilane column, named as Zorbax SB-C18 (5 µm, 4.6 x 150 mm) (Agilent Tech, USA) at 35 ± 0.5 ^{o}C. The mobile phase was water:acetonitrile:acetic acid mixture (34.5:65:0.5, v/v/v) run at a flow rate of 1 mL/min at 25 ^{o}C. The sample volume was 10 µL and quantification was performed at 280 nm using the instrument's software (Agilent Chem Station Rev. B. 04.03-SP2-105) to control the components of the instrument, to obtain and keep the virtual datum. The ICH Q2 (R1) guideline were followed for the method validation studies (20).

Preparation of lipid nanoparticles

Lipid nanoparticle (SLN and NLC) formulations were produced by hot homogenization and ultrasonication method at 80 ^{o}C (Table I) (18). Cetyl stearyl alcohol, Compritol® 888 ATO, oleic acid, and Lutrol® F68 were chosen as solid or liquid lipids and the surfactant. The solid lipid and the drug were dissolved in 5 mL methanol with a vortex mixer (IKA, Germany) for production of drug loaded SLN formulations. Methanol was removed by using a rotary evaporator (Heidolph, Germany) and the drug-loaded lipid layer was melted by heating at 80°C. The hot aqueous surfactant solution was added to the melt in a water bath (Isolab, Germany) and the mixture was homogenized under 10.000 rpm high-shear stirring at 80°C for 10 min. The hot coarse emulsion was then sonicated using a probe sonicator (Bandelin, Sonopuls, Germany) at 75% amplitude for 7 min. In the case of drug loaded NLC production, liquid lipid was added to the lipid phase reducing the fraction of solid lipid (1.5:3.5, w/w), i.e., the total lipid content stayed unchanged. Placebo SLN and NLC were also produced under the same conditions. Formulations were transferred into silanized vials and tightly sealed.

Table I Compositions of placebo and drug loaded formulations

Formulations		Constituents (% w/v)					
		Drug (LE)	Cetyl stearyl alcohol	Compritol® 888 ATO	Oleic acid	Lutrol® F68	Deionized Water
Placebo	CA-SLN	-	5	-	-	4	91.00
	CA-NLC	-	3.5	-	1.5	4	91.00
	Comp-SLN	-	-	5	-	3	92.00
	Comp-NLC	-	-	3.5	1.5	3	92.00
Drug loaded	LE-CA-SLN	0.05	5	-	-	4	90.95
	LE-CA-NLC	0.05	3.5	-	1.5	4	90.95
	LE-Comp-SLN	0.05	-	5	-	3	91.95
	LE-Comp-NLC	0.05	-	3.5	1.5	3	91.95
LE: Loteprednol etabonate							

Characterization of Formulations

Particle Size Analysis

Particle size and polydispersity index (PI) of nano particulate formulations were measured by the dynamic light scattering (DLS) method by using a Malvern Zetasizer Nano ZS (Malvern Instruments, UK) (22). Before the analysis, formulations were diluted with water (1:20, v:v) and then transferred into disposable polystyrene cuvettes.

Surface Morphology

Morphological assessment of the nanoparticles was performed by using a scanning electron microscope (SEM) (Zeiss EVO 40, USA). Before the SEM analysis, the formulations were freeze-dried by using a lyophilizer (Alpha 2-3 LO, Christ, USA) (23). Then, they were subjected to a gold coating process and micrographs were captured by using different magnifications of the SEM.

Encapsulation Efficiency and Loading Capacity Measurements

Drug encapsulation efficiency (EE) and drug loading capacity (LC) are critical quality attributes for SLN and NLC formulations. EE was calculated indirectly by detecting the amount of the free drug in the continuous medium of SLN and NLC (17, 24). The unencapsulated drug was isolated by the filtration and centrifugation method at 5000 rpm for half an hour, using filter units containing centrifuge tubes (Amicon® Ultra-4, Merck, Germany). The tubes consisted of a filter membrane with a molecular cut-off 300 kDa Amount of free drug in supernatants was detected by HPLC. EE and LC were determined by using the equations:

$$EE = [(A_{\text{initial drug}} - A_{\text{free drug}})] \times 100$$

$$LC = [(A_{\text{initial drug}} - A_{\text{free drug}}) / A_{\text{lipid}}] \times 100$$

Where "$A_{\text{initial drug}}$", "A_{lipid}" and "$A_{\text{free drug}}$" are amounts of initial drug and lipid used to prepare nanoparticles, and amount of free drug determined in the supernatant, respectively.

Fourier Transform Infrared Spectroscopy

The possible interactions between active ingredients and excipients of the formulation were detected by Fourier transform infrared spectroscopy (FT-IR). The formulations were lyophilized before the FTIR analysis (17). Samples obtained from placebo and drug loaded formulations, and pure LE were individually analyzed in range of 4000 to 650 cm^{-1} wavelength in the transmission mode in a Nicolet iS50 FT-IR (Thermo Scientific, USA) equipped with Omnic Version 9.0.0 Software.

Determination of Thermal Behaviors of Formulations

Differential scanning calorimetry (DSC) was performed on pure lipid and drug loaded formulations to determine the crystallization behavior of the lipid and the possible active ingredient - excipient interaction. Samples (25 µL) equal to 3-4 mg solid content were prepared into standard aluminium pans of the DSC apparatus (DSC 131, Setaram, France). The samples were heated from 25 ^{o}C to 200 ^{o}C with a heating rate of 10 ^{o}C /min under a nitrogen flow (20 mL/min). The thermogram was obtained using the Setsoft 2000 software. The crystalline state of the solid lipid in preparations was shown by the calculation of crystallinity (25). It was shown by calculation of crystallinity indices (CI) using the following equation:

$$CI\ (\%) = [ME_s / (ME_p \times C_d)] \times 100$$

Where ME_s and ME_p are melting enthalpy (J/g) of the sample and pure solid lipid, respectively. C_d concentration of the solid lipid (%).

Stability Study

Placebo and loaded formulations were kept at room temperature in the dark. The stability study has been performed over 3 months. At regular time intervals, samples were taken to determine their drug payload, particle size and zeta potential, and thermal behaviours of lipids in nanoparticles (26).

In vitro Release Study

The determination of *in vitro* release profiles of formulations was achieved by using Franz diffusion cells (Permegear, USA). The diffusion area of Franz diffusion cell was 2.88 cm^2 and a receptor volume was 20 mL. The release study was conducted under the sink conditions (27). 2 mL of formulations were put into donor chamber separated with an artificial membrane (Spectra/Por® Dialysis membrane, U.S.A with Mw cut-off at 3.5 kDa) from receiver chamber. At specified periods, 1 mL samples were taken from the release medium (PBS) then replenished by volume equivalent of fresh medium (28). HPLC method was applied for the quantification of samples.

Mathematically different release kinetics were investigated to determine the release profile. First order, Zero order, Higuchi and Korsmeyer-Peppas models were tested. A saturated solution of LE in the receptor medium (PBS) was also used for the release study as a control.

Ex vivo Permeation Study

Ex vivo permeation study of LE formulations was carried out on porcine skin (back area) using Franz diffusion cells. Our study was modified from Gupta and Trivedi's study with minor modifications (29). The porcine skin which is approximately 700 µm thickness was separated from the fat layer by blunt dissection (30). Skin samples were placed between the receptor and donor compartments of Franz diffusion cells with the dermal side in contact with the receptor medium and the epidermis side in contact with the donor chamber. 2mL SLN and NLC samples were placed in the donor compartment of the cells. A saturated solution of LE in the receptor medium (PBS) was also applied as the control. The receptor phase was kept at 32 ± 0.5°C under constant stirring at 160 rpm in accordance with the sink condition. Samples of 1 mL were taken from the receptor phase at pre-determined time intervals for 24 h and replenished by a volume equivalent of fresh PBS at the same thermal conditions. The HPLC analysis was performed in triplicate (31, 32).

Skin Retention and Deposition Study

Tape Stripping

A previously published tape stripping method was applied to measure LE amount in the *Stratum corneum* (33). At the end of the *ex vivo* study, the skins were recovered from the receptor chamber of Franz cell and excess formulation carefully removed using cotton buds and washed with PBS. After the washing process, regular sellotape (Ve-Ge®, Turkey) pieces were applied over the skin. After that, a light pressure was applied then they were removed. The first two applications were excluded as they typically contain formulation lodged within the crevices of the skin surface, rather than being deposited within the tissue. Fifteen sequential tape strips were used to separate the *Stratum corneum* from epidermis and dermis, 15 pieces were extracted in tubes containing 10 mL of acetonitrile:PBS mixture (75:25, v/v). An orbital shaker (bioSAN, S20-60, Riga, Latvia) was used for extraction for 24hours (34, 35). The strips were then

removed, and solution was evaporated with rota evaporator (Heidolph, Germany) and residue was reconstituted with 2 mL PBS. Sample was vortex 5 min then transferred to an autosampler vial (Agilent, 1.5 mL, USA), before being analyzed for LE by HPLC.

The remaining skin was divided into tiny pieces, placed into tubes (Heidolph, 20 mL, Germany) containing 5 mL of acetonitrile:PBS mixture (75:25, v/v). After that, the preparation was homogenized using a tissue homogenizer (Silent Crusher S, Heidolph, Germany, 1000 rpm) with 7 F probe for 5 mins. Then it was vortexed for 1 min, sonicated for 20 min, centrifuged for 5 min at 3000 rpm. The final preparation was filtered through a 0.45 µm pore membrane. The LE amount in the filtrate was determined by using HPLC (34, 36).

Statistical Analysis

One-way ANOVA (GraphPad® Prism (version 9.0.0) software) was used as statistical tool for some of the characterization studies, *in vitro* and *ex vivo* studies. $p \leq 0.05$ was set as the degree of significance to detect differences between mean data.

Results And Discussion

Preparation of the Formulations

The solubility of LE in different lipids is given in Table II. LE showed high solubility in Compritol® ATO 888 (0.11207 mg/mL), followed by cetyl stearyl alcohol (0.08084 mg/mL), Compritol® E ATO (0.04144 mg/mL) and 1-tetradecanol (0.04009 mg/mL). Compritol® ATO 888 is a blend of two different esters of behenic acid with glycerol (37). Cetyl stearyl alcohol is a mixed lipid consisting of the combination of long carbon rings of cetyl and stearyl alcohol. This lipid allows the polar molecules present in surfactants to form a bilayer structure with the outer surface molecules. This bilayer structure can provide a higher rate of drug entrapping capacity by reducing the possibility of lipid crystallization. In addition to this advantage, since the molecules in the polar part of cetyl stearyl alcohol cause a high rate of water retention in their outer structure, a tendency to gel can also be seen. (38). In classical emulsions prepared after lipid imaging study, a fluid formulation without phase separation in Compritol® ATO 888 and cetyl stearyl alcohol was obtained. Shimojo et al., in which NLC loaded with resveratrol were formulated, Compritol® ATO 888 as solid lipid, Miglyol® 812 as liquid lipid, and poloxamer® 188 as a surfactant were used in varying proportions. They reported that there was no phase separation in the classical emulsions they prepared after the solubility studies (39). In another study, compritol was used to obtain dexamethasone-loaded SLN particles because it dissolves the active substance at a high rate (0.08388 mg/ mL) and forms a fluid emulsion (40). In a study by Vieira et al., NLC formulations prepared which containing cetyl stearyl alcohol with various lipids (Imwitor® 900K, Kolliwax® GMS II and Dynasan® 116) as solid lipids and sucupira oil as oil. It has been reported that formulations prepared using cetyl stearyl alcohol are more fluid and maintain their homogeneity (41). The uniformity and homogenicity of SLN and NLC prepared using cetyl stearyl alcohol and Compritol® 888 ATO were also attributed to the efficiency of the emulsion step.

Table II Solubility of LE in different lipids, oils, and surfactants

Solid Lipids	Solubility of the drug (mg/mL)
1-tetradecanol	0.04009^{c} ±0.0011
Cetyl alcohol	0.04322^{c} ±0.0014
Cetyl palmitate	0.04811^{c}±0.0017
Cetyl stearyl alcohol	0.08084^{b}±0.0019
Compritol® E ATO	0.04144^{c}±0.0017
Compritol® 888 ATO	0.11207^{a}±0.0022
Cutina® CP	0.04716^{c}±0.0010
Geleol™	0.04763^{c}±0.0013
Gelucire® 50/13	0.04311^{c}±0.0024
Imwitor® 491	0.04877^{c}±0.0020
Imwitor® 900K	0.04664^{c}±0.0014
Nacol® 16-98	0.04407^{c}±0.0017
Softisan® 141	0.04729^{c}±0.0023
Softisan® 601	0.04308^{c}±0.0018
Stearic acid	0.05114^{c}±0.0021
Oils	
Castor oil	0.05812^{b}±0.0015
Isopropyl myristate	0.06899^{b}±0.0022
Oleic acid	0.09977^{a}±0.0012
Olive oil	0.05707^{b}±0.0017
Surfactants	

(a-c): Statistically different between the other component ($p \leq 0.05$)

Solid Lipids	Solubility of the drug (mg/mL)
Cremephor EL®	0.09105^{b}±0.0014
Cremephor® RH 40	0.09983^{b}±0.0019
Labrasol®	0.12039^{b}±0.0017
Lutrol® F68	0.16328^{a}±0.0020
Tween® 80	0.10116^{b}±0.0016
(a-c): Statistically different between the other component ($p \leq 0.05$)	

LE showed high solubility in oleic acid (0.09977 mg/mL), followed by isopropyl myristate (0.06899 mg/mL), castor oil (0.05812 mg/mL) and olive oil (0.05707 mg/mL). While formulations prepared using oleic acid were stable at room temperature, it was observed that phase separation and precipitation occurred after a while in formulations prepared using other oils, which supports the effect of oleic acid in the formation of a homogeneous colloidal system. Prado Almeida et al. prepare lipid based nanoparticles which contained oleic acid was preferred as a liquid lipid due to its high solubility of the active substance (0,167 mg/mL) and it was reported that the formulations prepared with stearyl alcohol did not undergo phase separation (42).

It has been observed that LE solubility in surfactants is higher than in oils and lipids. LE showed high solubility in Lutrol® F68 (0.16328 mg/mL); subsequent to Labrasol® (0.12039 mg/mL), Tween® 80 (0.10116 mg/mL), Cremephor® RH40 (0.9983 mg/mL) and Cremephor® EL (0.9105 mg/mL). Following the solubility study in surfactants, conventional emulsions were prepared with surfactants. While no phase separation was observed in formulations using p as surfactant, phase separation was observed in other formulations. In a study by Leonardi et al., Lutrol F68 as surfactant and other surfactants (Tween® 80, Cremophor® A25, Lipoid® S100, and Kolliphor® HS) are present in varying proportions in the prepared SLN. It was observed that the lowest particle size and distribution of the prepared SLN formulations belonged to the formulation containing 2% (w/v) Lutrol® F68 (213.8, 0.182), while the formulation that

maintained its physical stability for the longest time during storage was the formulations containing Lutrol® F68 (43). These findings show that Lutrol® F68 may be a suitable choice of surfactant for SLN and NLC formulations to be prepared. Generally, phase separation or aggregation was not encountered in all formulations prepared.

It was confirmed that optimal SLN and NLC formulations by choosing Lutrol® F68 as the surfactant, Compritol® 888 ATO, and cetyl stearyl alcohol as lipid and oleic acid as oil.

Measurement of LE amount and Analytical Method Validation

The retention time of LE was found to be 7.14 min (Fig. 1A). In the HPLC chromatogram obtained from the mobile phase, no peaks were observed in the mobile phase that could interfere with the LE peak (Figure 1B). In the peak of LE, there was no interference to the peaks of the other components used in the formulations and showing the specificity of the method (Figure 1). Linearity validation was performed with a standard calibration curve in the range 100–5000 ng/mL prepared from the stock solution of LE (1µg/mL). The equation of the regression created as a result of the calibration was calculated as y = 0.0253x + 0.2144 (r^2=0.9906). It was observed that the relative standard deviations of the validation parameters of the method for accuracy, intra-day and inter-day precision were below 2%. While the recycling percentages of LE were determined as 93.57 ± 0.11 – 96.27 ± 0.19%, limit of detection (LOD) and limit of quantification (LOQ) were found to be 18.66 ng/mL and 54.82ng/mL, respectively.

Solubility Study

The solubility of LE in water and PBS was determined as 6.1913 ± 0.0008 µg/mL and 1.1122 ± 0.0005 µg/mL at 25 ± 1 ^{o}C, respectively.

Characterization of Formulations

Particle Size Analysis

Particle size analysis showed that formulations had particles in the range of 100–150 nm in average (Figs. 2 and 3). Polydispersity index (PI) values of less than 0.200 indicated that the formulations had a homogeneous and narrow particle size distribution (21, 22). The lowest particle size was obtained with formulation Comp-NLC (134.1 nm, 0.138 PI), while Comp-SLN (140.8 nm, 0.159 PI), Ca-NLC (141.7 nm, 0.199 PI) and Ca-SLN (143.9 nm, 0.168 PI) respectively followed this formulation. Incorporation of the drug did not remarkably increase the particle size of the formulations. It was obvious that the particle size of LE-Comp-NLC did not change significantly during 3 months of storage ($p > 0.05$), while the particle size of other formulations increased statistically ($p \leq 0.05$). Formulation LE-CA-NLC displayed the highest increase from 143.9 nm (0.248 PI) to 155.6 nm (0.269 PI). Although statistical evaluations showed an increase in these formulations but not remarkable. No microparticle content or agglomeration was detected in all formulations during 3 months of storage.

In general, zeta potential of the formulations was between (-22.4) - (-24.8) and it did not significantly change over 3 months ($p > 0.05$). It was observed that the zeta potential of the drug loaded formulations was higher but exhibited insignificant difference compared to placebo formulations ($p > 0.05$).

SEM Analysis

SEM images provided information on the morphologies and particle sizes of CA-NLC, LE-CA-NLC, CA-SLN, LE-CA-SLN, Comp-NLC, LE-Comp-NLC, Comp-SLN and LE-Comp-SLN formulations. (Figure 4). When the DLS and SEM data were compared, it was concluded that they were consistent with each other, and it was proven that the lipid colloid systems did not contain micro-structured particles and crystallization signs of the active substance.

Encapsulation Efficiency and Drug Loading Capacity

EE of LE-CA-SLN, LE-CA-NLC, LE-Comp-SLN and LE-Comp-NLC was found to be 72.03 ± 0.78%, 77.82 ± 0.44%, 75.08 ± 0.22% and 79.03 ± 0.54%, respectively (Fig. 5). LC of formulations was 6.548 ± 0.0029%, 7.075 ± 0.0041%, 6.825 ± 0.008% and 7.185 ± 0.0017% in the same order. Type of surfactant, oil or solid lipid content, and amount of the drug have been stated as critical attributes that have impact on EE and LC of lipid nanoparticle formulations (22). Results demonstrated that oil amount was critical for EE and LC. The length of the behenic acid ester chain of Compritol® 888 ATO allowed more drug molecules to be trapped, resulting in higher EE (LE-Comp-NLC) compared to formulation containing cetyl stearyl alcohol (LE-CA-NLC) (37).

The negatively charged groups in the hydrocarbon tail of CA interact with the positive groups of the drug molecule and may have a negative effect on EE (37, 38).

The addition of liquid lipid to the formulation caused the ordered structure from solid lipid to become disordered. This irregular structure resulted in more drug entrapment in the formulation, resulting in an increase in EE and LC values. At the same time, the liquid lipid also reduces the crystallization that occurs in the formulation formed with the solid lipid, allowing the drug to be substituted in the formulation stably for a longer period of time. Developed as an alternative to SLN, NLC help the stable crystal structure of the solid lipid deteriorate and remain in the amorphous structure, helping the drug to be found in these amorphous structures (25).

Statistically, the results are demonstrated that, there is no significant difference on the EE and LC values of the formulations between PD and 3 months ($p > 0.05$). Unchanged EE and LC values indicated that the drug was not expulsed from the nanoparticles during storage.

FT-IR Analysis

FT-IR was used to see the physical and chemical interactions between the active ingredient and other ingredients. As shown in Figure 6, the intensity of characteristic spectra for LE was detected at much lower intensity and wider peaks than those caused by the other components. Tensile bands due to C=O vibrations arising from the ester structure in triglycerides caused sharp peaks to be seen at 1831.09–

1559.54 cm^{-1}, 886.131-1289.18 cm^{-1} and 743.224 cm^{-1} (C–Cl stretch band). In addition to the bands originating from the vibrations of the acetyl group found in LE, bands originating from the C-H and O-H vibrations of the triglyceride group were detected at 2921.71–2818.96 cm^{-1}. Similar results have been reported in various studies (44–46). In formulations containing Compritol®888 ATO, two main peak spectra were observed at 1815 cm^{-1} and 1706 cm^{-1} due to the C=C stretching and the vibrations of the -OH group (C=C stretching and normal OH stretching, respectively) (47). In drug-loaded formulations, these peaks seem to disappear due to drug-related peaks (1831.09–1559.54 cm^{-1}).

For CA-SLN and CA-NLC the main peak for % transmittance is observed at 2800-2600 cm^{-1} which was identified to C–H group, however, this peak was observed as shifted at 2800-2600 cm^{-1} for LE-CA-SLN and LE-CA-NLC formulations. Another major peak for the bands from 1708–1738 cm^{-1}, which corresponds to the C=O group, and from 1586–1604 cm^{-1} corresponding to the C=C group, were observed in all the excipient spectra (48). Also, the peak between 870.06-610.18 cm^{-1} (C-O stretch) seen in all formulations except the pure LE is highly likely to be caused by Lutrol® F68. (49). It was concluded that there was no interaction between the active ingredient and excipients.

Thermal Behaviors of Formulations

The melting point of plain Compritol® 888 ATO was found as 74.94 ^{o}C with 225.16 J g^{-1} melting enthalpy (Fig. 7) (Table III). Comp-SLN yielded a melting peak at 70.41 ^{o}C with a melting enthalpy of 37.526 J g^{-1}. CI was calculated as 50.81%. CA-SLN yielded a melting peak at 71.88 ^{o}C with a melting enthalpy of 29.833 J g^{-1} due to the addition of surfactant to the dispersion (25). CI was calculated as 39.38%. The reduction in obtained initial and peak temperatures, which is evident in NLCs, may be due to the reduction in size. The fact that the melting range is lower than pure lipids can be explained by the transformation of the formulation towards an amorphous structure (50). The appearance of the amorphous structure can be attributed to the disruption of the ordered lattice structure of the solid lipid with much lower energy than the enthalpy that would be spent. Therefore, the result was obtained that the liquid lipid resulted in a lower lattice arrangement compared to the formulation containing the solid lipid. NLC formulations were attributed to the presence of liquid lipid incorporation resulting in delayed crystallization of nanoparticles. According to table 4, 67.58 ^{o}C and 27.772 J g^{-1} 71.82 ^{o}C melting enthalpies were obtained from Comp-NLC and LE-Comp-NLC. For formulations containing CA; 21.766 J g^{-1} and 24.091 J g^{-1} melting enthalpies were obtained from CA-NLC and LE-CA-NLC, resulting in 36.85 and 39.34% CI, respectively.

Incorporation of the drug in Comp-SLN induced the melting point and melting enthalpy. resulting in a remarkable decrease in CI. SLN based on CA, gave a double peak at 74.26 and 75.11 ^{o}C, which could be attributed to the mixture of cetyl alcohol and stearyl alcohol in CA (Fig. 7) (25). Similar behaviours were detected with CA based SLN formulations as can be seen in Table III.

Table III DSC parameters of formulations and formulation components after three months at room temperature.

Formulation	Storage (RT)	Melting enthalpy ΔH (J/g)	Melting point (°C)	CI (%)
Bulk Cetyl stearyl alcohol	-	225.16	74.94	-
Bulk Compritol ATO888	-	192.23	78.23	-
CA-SLN	1st day	29.833	71.88	39.38
	60th day	30.248	72.21	40.86
	90th day	30.533	72.74	41.68
LE-CA-SLN	1st day	34.814	73.86	43.47
	60th day	37.018	74.47	44.14
	90th day	36.99	73.77	44.59
CA-NLC	1st day	21.766	70.47	36.85
	60th day	22.912	71.13	37.72
	90th day	25.942	71.44	37.91
LE-CA-NLC	1st day	24.091	72.91	39.34
	60th day	26.259	72.96	39.93
	90th day	26.295	71.29	40.16
Comp-SLN	1st day	37.526	70.41	50.81
	60th day	37.564	71.38	51.07
	90th day	37.640	72.09	51.56
LE-Comp-SLN	1st day	37.886	74.21	53.24[a]
	60th day	38.050	72.38	54.36[b]
	90th day	38.110	72.56	54.73[c]
Comp-NLC	1st day	23.427	67.58	43.39
	60th day	22.65	69.62	44.8
	90th day	26.685	68.5	45.13
LE-Comp-NLC	1st day	27.772	71.82	45.72
	60th day	26.851	72.91	46.24

CI: crystallinity indice

Formulation	Storage (RT)	Melting enthalpy ΔH (J/g)	Melting point (°C)	CI (%)
	90th day	26.990	73.16	47.16
CI: crystallinity indice				

In vitro Release Study

The cumulative percent release of LE from formulations (LE-Comp-SLN, LE-Comp-NLC, Control, LE-CA-SLN and LE-CA-NLC) was monitored for 8 hours. Each sample was analyzed six times. The outcomes are demonstrated in Fig. 8. It was found that, the concentration of the drug in the formulation directly affected the release rate. LE-Comp-SLN, LE-Comp-NLC, LE-CA-SLN and LE-CA-NLC displayed sustained drug release. LE release was the lowest with SLN followed by NLC as can be seen in Figure 7 ($p < 0.05$). The release rate of LE from the different formulations was 1.731 ± 0.017, 2.295 ± 0.015 2.389 ± 0.019 and 4.186 ± 0.022 mcg/mL/h. It was found out that Control LE solution released 100% of LE at the end of 2h while LE-Comp-NLC, LE-CA-NLC, LE-Comp-SLN and LE-CA-SLN released 69.71%. 64.11%. 64.06% and 59.51% of the drug respectively. In the control group, there was a significant difference between SLN and NLC formulations, as well as between SLN and NLC formulations. ($p<0.05$). In general, it was found that the release rate of LE increased due to the decrease in the %CI values of SLN and NLC (16,17). Addition of liquid lipid to SLN based on CA (LE-CA-NLC) brought out more shortcomings compare to SLN based on Compritol®888 ATO (LE-Comp-SLN).

The release profiles of the formulations were found to be in accordance with the Korsmeyer-Peppas release model (Table IV). In addition, since the n value (0.442) calculated in the Korsmeyer-Peppas model was lower than 0.45, it was found to be suitable for Fickian diffusion release (state I diffusional) for LE-CA-SLN (Table IV) (17.25). Since the n values of LE-Comp-NLC and LE-CA-NLC formulations (0.4792 and 0.4738, respectively) were between $0.45 \leq n \leq 0.89$, both diffusional and erosional drug release was observed and proved to be suitable for non-Fickian release. Considering the evaluations of LE-Comp-NLC and LE-CA-NLC formulations in terms of both in vitro release study and release kinetics, it is clear that the way of drug encapsulation results in amorphous or defective drug structure. Beside of that drug release from LE-Comp-SLN and control followed Higuchi type kinetic model with non-Fickian anomalous transport as indicated by Korsmeyer-Peppas model.

Table IV: Mathematical assessment of drug release from formulations.

Formulations	Zero order. R	First order. R	Hixson-Crowell. R	Higuchi. R	Korsmeyer-Peppas. R (n)
LE-Comp-SLN	0.9338	0.8253	0.9103	0.9957	0.9946 (0.4571)
LE-Comp-NLC	0.9486	0.8529	0.9227	0.9841	0.9982 (0.4792)
LE-CA-SLN	0.9266	0.8127	0.9055	0.9902	0.9932 (0.4421)
LE-CA-NLC	0.9471	0.8463	0.9108	0.9812	0.9973 (0.4738)
Control	0.7386	0.6944	0.9016	0.9605	0.9117 (0.3612)

Ex vivo Permeation Study

SLNs and NLCs were reported as penetration enhancers in several studies (17). SLN and NLC formulations were increased the penetration rate of LE when compared with the control group ($p \leq 0.05$). There is no remarkable difference between LE-Comp-SLN and LE-CA-SLN formulations ($p > 0.05$). The steady-state flux achieved by drug penetration was different between the control LE and nanoparticles. It was observed between 2- 6 h for LE-Comp-SLN, LE-Comp-NLC, LE-CA-SLN and LE-CA-NLC and between 0-4 hours for control LE. The steady-state flux achieved by drug penetration was different between the control LE and nanoparticles. It was observed between 4 and 8 hours for LE-Comp-SLN, LE-Comp-NLC, LE-CA-SLN and LE-CA-NLC and between 1 and 4 hours for control LE. In those periods steady state flux values were 52.998 $\mu g.cm^{-2}\ h^{-1}$. 57,835 $\mu g.cm^{-2}\ h^{-1}$. 52,109 $\mu g.cm^{-2}\ h^{-1}$. 53,232 $\mu g.cm^{-2}\ h^{-1}$. and 26,623 $\mu g.cm^{-2}\ h^{-1}$ LE-Comp-SLN, LE-Comp-NLC, LE-CA-SLN, LE-CA-NLC and control, respectively (Fig. 9). It is observed that there is a statistically significant difference the flux value of the LE-Comp-NLC formulation compared to LE-Comp-SLN, LE-CA-SLN, LE-CA-NLC and control group ($p \leq 0.05$).

Tape Stripping Study

Extraction of the drug from the porcine skin followed by tape stripping and skin homogenization process was performed for nanoparticles and control group; the results are showed in Fig. 10. The values of LE obtained from LE-Comp-SLN, LE-Comp-NLC, LE-CA-SLN, LE-CA-NLC and control were 0.1699 mg (2.53%), 0.1617 mg (2.11%), 0.1661 mg (2.88%), 0.1632 (2.38%) and 6.693 mg (67.79%) in the SC and 3.236 mg (47.16%), 3.985 mg (49.11%), 3.112 mg (45.29%), 2.666 mg (46.62%) and 0.243 mg (2.43%) in the viable skin layers (epidermis and dermis) and 3.928 mg (52.36%), 4.083 mg (51.67%), 3.690 mg (47.42%), 3.699 mg (47.42%) and 2.971 mg (29.22%) in the donor compartment. respectively. It was observed that there was no statistically significant difference between LE-Comp-SLN, LE-Comp-NLC, LE-CA-SLN and LE-CA-NLC in terms of LE amount in SC ($p > 0.05$). Besides of that, when examined in terms of the amount of cumulative LE in donor phase and the amount of LE in viable dermis, it is seen that LE-Comp-NLC has statistically significant difference from other formulations ($p \leq 0.05$).

Overall NLC formulations exhibited higher penetration enhancer effect than SLN. LE-Comp-NLC exhibited the highest retention of LE in the deeper parts of the skin. For LE-Comp-NLC formulation 49.11% of the total amount of LE that penetrated from the skin was held in the epidermis and dermis. This amount was remarkably higher than control group ($p \leq 0.05$) but not significant with LE-CA-NLC and LE-CA-SLN formulations ($p>0.05$).

Additionally, Compritol® 888 ATO based nanoparticles escaped to the deeper layers due to advantageous nanometer size. Moreover, spontaneous occlusion of lipid nanoparticles contributed to the penetration properties through the skin. Subsequent skin hydration can be a reason of promoted drug penetration (25, 51).

Conclusion

SLN and NLC of LE were perfectly prepared with high drug loading capacity using Compritol® 888 ATO, CA and oleic acid as solid and liquid lipids. The drug load of SLN and NLC was high as the lipid colloidal system was desired. Addition of liquid lipid to the formulation resulted in an increase in drug loading capacity compared to SLN. Stability studies have proven that the formulations are physically stable and that there is active substance-excipient compatibility during 90 days of storage. It has been proven that SLN and NLC formulations increase the penetration rate of the drug into the skin 20-30 times compared to the control group, acting as a depot for the viable skin to provide sustained drug release. As a result, it was concluded that topically developed SLN and NLC formulations of LE would be an advantageous alternative in the treatment of all kinds of inflammatory and allergic conditions of the skin.

Abbreviations

CA	Cetyl Stearyl Alcohol
DLS	Dynamic Light Scattering
DSC	Differential Scanning Calorimetry
EE	Entrapment Efficiency
LC	Loading Capacity
FT-IR	Fourier Transform Infrared Spectroscopy
HPLC	High Performance Liquid Chromotography
LE	Loteprednol Etabonate
NLC	Nanostructure Lipid Carrier
SEM	Scanning Electron Microscopy

SLN	Solid Lipid Nanoparticle
PD	Production Day

Declarations

CONFLICT OF INTEREST

The authors declare that there is no conflict of interest.

ACKNOWLEDGMENTS

The authors would like to thank Dr. Pınar Akkuş for providing the electron microscopy laboratories.

AUTHOR CONTRIBUTIONS

Conception: BÜ, SÖ; Design: BÜ, SÖ, MÜ; Supervising: SÖ, ÇT, MÜ, YE; Resources: BÜ, ÇT; Materials: BÜ, SÖ, ÇT; Data collection: BÜ, SÖ; Interpretation; SÖ, MÜ, ÇT; Literature search: BÜ, SÖ, MÜ; Writing manuscript; BÜ, SÖ, MÜ; Critical review: MÜ, ÇT, YE.

References

1. Goldstein BG, Goldstein AO. Dellavelle, R.P. and Levy. M.L., editors, Topical corticosteroids: Use and adverse effects. Topical corticosteroids, 2021: Up to Date.
2. Rathi SK, D'Souza P. Rational and ethical use of topical corticosteroids based on safety and efficacy. Indian J Dermatol., 2012;57(4):251–259.
3. Das A, Panda S. Use of Topical Corticosteroids in Dermatology: An Evidence-based Approach. Indian J Dermatol., 2017;62(3):237–250.
4. Fong R, Cavet ME, DeCory HH, Vittitow JL. Loteprednol etabonate (submicron) ophthalmic gel 0.38% dosed three times daily following cataract surgery: integrated analysis of two Phase III clinical studies. Clin Ophthalmol., 2019;13:1427–1438.
5. Comstock TL, Sheppard JD. Loteprednol etabonate for inflammatory conditions of the anterior segment of the eye: twenty years of clinical experience with a retrometabolically designed corticosteroid. Expert Opinion on Pharmacotherapy, 2018;19(4):337–353.
6. Noble S, Goa KL. Loteprednol etabonate. BioDrugs, 1998:10(4), 329–339.
7. Alberth M, Wu WM, Winwood D, Bodor, N. Lipophilicity, solubility and permeability of loteprednol etabonate: a novel, soft anti-inflammatory steroid. J Biopharm Sci, 1991;2(2): 115–125.
8. Jensen LB, Petersson K, Nielsen HM. In vitro penetration properties of solid lipid nanoparticles in intact and barrier-impaired skin. European Journal of Pharmaceutics and Biopharmaceutics. 2011;79(1):68–75.

9. Patra JK, Das G, Fraceto LF, Campos EVR., Rodriguez-Torres M, Acosta-Torres LS., et al. Nano based drug delivery systems: recent developments and future prospects. Journal of nanobiotechnology, 2018;16(1):1–33.
10. Korting HC, Schäfer-Korting M. Carriers in the topical treatment of skin disease. Drug delivery, 2010:435–468.
11. Ramadon D, McCrudden MT, Courtenay AJ, Donnelly RF. Enhancement strategies for transdermal drug delivery systems: Current trends and applications. Drug Delivery and Translational Research, 2021;1–34.
12. Uchechi O, Ogbonna JD, Attama AA. Nanoparticles for dermal and transdermal drug delivery. Application of nanotechnology in drug delivery, 2014;4:193–227.
13. Naseri N, Valizadeh H, Zakeri-Milani P. Solid lipid nanoparticles and nanostructured lipid carriers: structure, preparation and application. Advanced pharmaceutical bulletin, 2015;5(3): 305.
14. Attama AA, Momoh MA, Builders PF. Lipid nanoparticulate drug delivery systems: a revolution in dosage form design and development. Recent advances in novel drug carrier systems, 2012;5:107–140.
15. Naseri N, Valizadeh H, Zakeri-Milani, P. Solid lipid nanoparticles and nanostructured lipid carriers: structure, preparation and application. Advanced pharmaceutical bulletin, 2015;5(3): 305.
16. Souto EB, Almeida AJ, Müller RH. Lipid nanoparticles (SLN®, NLC®) for cutaneous drug delivery: structure, protection and skin effects. Journal of Biomedical Nanotechnology, 2007;3(4):317–331.
17. Üner M, Yener G, Erguven E, Karaman EF, Utku EG. Solid Lipid Nanoparticles and Nanostructured Lipid Carriers of Celecoxib for Topical Application – Preparation. Characterization and Drug Penetration Through Rat Skin. Current Nanoscience. 2014;10(4):532–542.
18. Khames A, Khaleel MA, El-Badawy MF, El-Nazhawy AOH. Natamycin solid lipid nanoparticles – sustained ocular delivery system of higher corneal penetration against deep fungal keratitis: preparation and optimization. International Journal of Nanomedicine. 2019;14:2515–2531.
19. Padhye SG, Nagarsenker MS. Simvastatin Solid Lipid Nanoparticles for Oral Delivery: Formulation Development and In vivo Evaluation. Indian J Pharm Sci. 2013;75(5):591–598.
20. Han Y, Segall A. A validated specific stability-indicating RP-HPLC assay method for the determination of loteprednol etabonate in eye drops. J Chromatogr Sci. 2014;53:761–766.
21. Özdemir S. Aldosteron antagonisti eplerenonun yeni formülasyonlarının geliştirilmesi üzerine çalışmalar. 2016: İstanbul Üniversitesi Sağlık Bilimleri Enstitüsü, İstanbul. TR.
22. Özdemir S, Çelik B, Türköz Acar E, Duman G, Üner M. Eplerenone nanoemulsions for treatment of hypertension. Part I: Experimental design for optimization of formulations and physical characterization. Journal of Drug Delivery Science and Technology. 2018;45: 357–366.
23. Bhalekar M., Upadhaya P., Madgulkar A. Formulation and characterization of solid lipid nanoparticles for an anti-retroviral drug darunavir. Appl Nanosci., 2017;7:47–57.

24. Üner M, Yener G, Ergüven M. Design of colloidal drug carriers of celecoxib for use in treatment of breast cancer and leukemia. Materials Science & Engineering: C, 2019;103: 109874.
25. Üner M, Karaman E, Aydoğmuş Z. Solid Lipid Nanoparticles and Nanostructured Lipid Carriers of Loratadine for Topical Application: Physicochemical Stability and Drug Penetration through Rat Skin. Tropical Journal of Pharmaceutical Research, 2014;13(5):653.
26. Siekmann B, Westesen K. Thermoanalysis of the recrystallization process of melt-homogenized glyceride nanoparticles. Colloid Surface B., 1994;3(3):159–175.
27. Ghadiri M, Fatemi S, Vatanara A, Doroud D, Najafabadi AR, Darabi M., et al. Loading hydrophilic drug in solid lipid media as nanoparticles: Statistical modeling of entrapment efficiency and particle size. Int J Pharm. 2012;424(1-2):128–137.
28. Ng S, Rouse J, Sanderson D, Gillian E. A Comparative Study of Transmembrane Diffusion and Permeation of Ibuprofen across Synthetic Membranes Using Franz Diffusion Cells. Pharmaceutics. 2010;2(2):209–223.
29. Gupta V, Trivedi P. Ex vivo localization and permeation of cisplatin from novel topical formulations through excised pig. goat. and mice skin and in vitro characterization for effective management of skin-cited malignancies. Artificial Cells, Nanomedicine and Biotechnology. 2015;43(6):373–382.
30. Olatunji O, Das D, Garland MJ, Belaid L, Donnelly R. Influence of Array Interspacing on the Force Required for Successful Microneedle Skin Penetration: Theoretical and Practical Approaches. Journal of pharmaceutical sciences. 2013;102(4):1209–1221.
31. Parra A, Clares B, Rosselló A, Garduño-Ramírez ML, Abrego, G., García ML., et al. Ex vivo permeation of carprofen from nanoparticles: A comprehensive study through human. porcine and bovine skin as anti-inflammatory agent. International Journal of Pharmaceutics. 2016;501(1-2):10–17.
32. International Conference on Harmonization (I.C.H.). Validation of analytical procedures.: Text and Methodology, Q2, vol 11. R1. 2005; Geneva, Switzerland.
33. Alsaqr A, Rasoully M, Musteata FM. Investigating Transdermal Delivery of Vitamin D3. AAPS PharmSciTech. 2015;16(4):963–972.
34. Houston DMJ, Bugert J, Denyer SP, Heard CM. Anti-inflammatory activity of Punica granatum L. (Pomegranate) rind extracts applied topically to ex vivo skin. European Journal of Pharmaceutics and Biopharmaceutics. 2017;112:30–37.
35. Kahraman E, Neşetoğlu N, Güngör S, Şehvar Ünal D, Özsoy Y. The combination of Nanomicelles with Terpenes for Enhancement of Skin Drug Delivery. International Journal of Pharmaceutics. 2018;551(1-2):133–140.
36. Pepe D, Carvalho V, McCall M, de Lemos D, Lopes L. Transportan in nanocarriers improves skin localization and antitumor activity of paclitaxel. Int J Nanomedicine. 2016;11:2009–2019.
37. Aburahma MH, Badr-Eldin SM. Compritol 888 ATO: a multifunctional lipid excipient in drug delivery systems and nanopharmaceuticals. Expert Opin Drug Deliv. 2014;11(12):1865–83.
38. Kar M, Chourasiya Y, Maheshwari R, Tekade RK. Current Developments in Excipient Science: Implication of Quantitative Selection of Each Excipient in Product Development. Basic Fundamentals

of Drug Delivery. 2019;29–83.

39. Shimojo AAM, Fernandes ARV, Ferreira NRE, Sanchez-Lopez E, Santana MHA, Souto EB. Evaluation of the Influence of Process Parameters on the Properties of Resveratrol-Loaded NLC Using 22 Full Factorial Design. Antioxidants. 2019;8(8): 272.
40. Chen G, Hou SX, Hu P, Hu QH, Guo DD, Xiao Y. In vitro dexamethasone release from nanoparticles and its pharmacokinetics in the inner ear after administration of the drug-loaded nanoparticles via the round window. Journal of Southern Medical University. 2008;28(6):1022–1024.
41. Vieira S, Severino P, Nalone L, Souto SB, Lucarini M, Souto EB. Sucupira Oil-Loaded Nanostructured Lipid Carriers (NLC): Lipid Screening, Factorial Design, Release Profile, and Cytotoxicity. Molecules. 2020;25(3):685.
42. Almeida EDP, Dipieri LV, Rossetti FC, Marchetti JM, Bentley MVL, Nunes RDS., et al. Skin permeation, biocompatibility and antitumor effect of chloroaluminum phthalocyanine associated to oleic acid in lipid nanoparticles. Photodiagnosis and photodynamic therapy. 2018;24:262–273.
43. Leonardi A, Bucolo C, Romano GL, Platania CBM, Drago F, Puglisi G, et al. Influence of different surfactants on the technological properties and in vivo ocular tolerability of lipid nanoparticles. International Journal of Pharmaceutics. 2014;470(1-2): 133–140.
44. Sahoo S, Khodakiya A, Mithapara C, Sahu AR, Vaidya SK. Formulation and evaluation of sustained release in situ gel of loteprednol etabonate by using 3 2 full factorial design. Aegaeum Journal, 2020;8(4):566.
45. Khandelmai NP, Bhide P, Nachinolkar R. Formulation and evaluation of solubility enhanced in situ gelling eye drops of loteprednol etabonate. AJPCR. 2019;12(12).
46. LGC GmbH. Certificate of Analysis Reference Standard Loteprednol Etabonate (TGZ II. D-14943). 2017; Luckenwalde, Germany.
47. Tatke A, Dudhipala N., Janga KY, Balguri SP, Avula B, Jablonski MM., et al. In situ gel of triamcinolone acetonide-loaded solid lipid nanoparticles for improved topical ocular delivery: Tear kinetics and ocular disposition studies. Nanomaterials. 2019;9(1):33.
48. Elmowafy M, Shalaby K, Badran MM, Ali HM, Abdel-Bakky MS, Ibrahim HM. Multifunctional carbamazepine loaded nanostructured lipid carrier (NLC) formulation. International journal of pharmaceutics. 2018;550(1-2):359–371.
49. De Oliveira EG, Machado PRL, Farias KJS, da Costa TR, Melo DMA, Lacerda AF, et al. Tailoring structural properties of spray-dried methotrexate-loaded poly (lactic acid)/poloxamer microparticle blends. Journal of Materials Science: Materials in Medicine, 2019;30(1).
50. Jia L, Zhang DR, Li Z., Feng FF, Wang YC, Dai WT, et al. Preparation and characterization of silybin-loaded nanostructured lipid carriers. Drug Delivery. 2009;17(1): 11–18.
51. Wissing SA, Lippacher A, Müller RH. Investigations on the occlusive properties of solid lipid nanoparticles (SLN). J. Cosmet. Sci. 2001;52:313–324.
52. How CW, Abdullah R, Abbasalipourkabir R. Physicochemical properties of nanostructured lipid carriers as colloidal carrier system stabilized with polysorbate 20 and polysorbate 80. African J

Biotechnol. 2011;10(9):1684–1689.

Figures

Figure 1

HPLC chromatograms of LE (A), mobile phase (B) and mixtures (C) CA:Lutrol® 68 mixture, (D) Compritol® 888 ATO: Lutrol® 68 mixture, (E) CA: Lutrol® 68:OA mixture, (F) Compritol® 888 ATO:Lutrol® 68:OA mixture.

Figure 2

Size distribution graphs taken from DLS analysis demonstrating particle size distribution of SLN and NLC formulations on the production day: (A) CA-NLC (B) CA-SLN, (C) Comp-NLC, (D) Comp-SLN (E) LE-CA-NLC, (F) LE-CA-SLN, (G) LE-Comp-NLC and (H) LE-Comp-SLN.

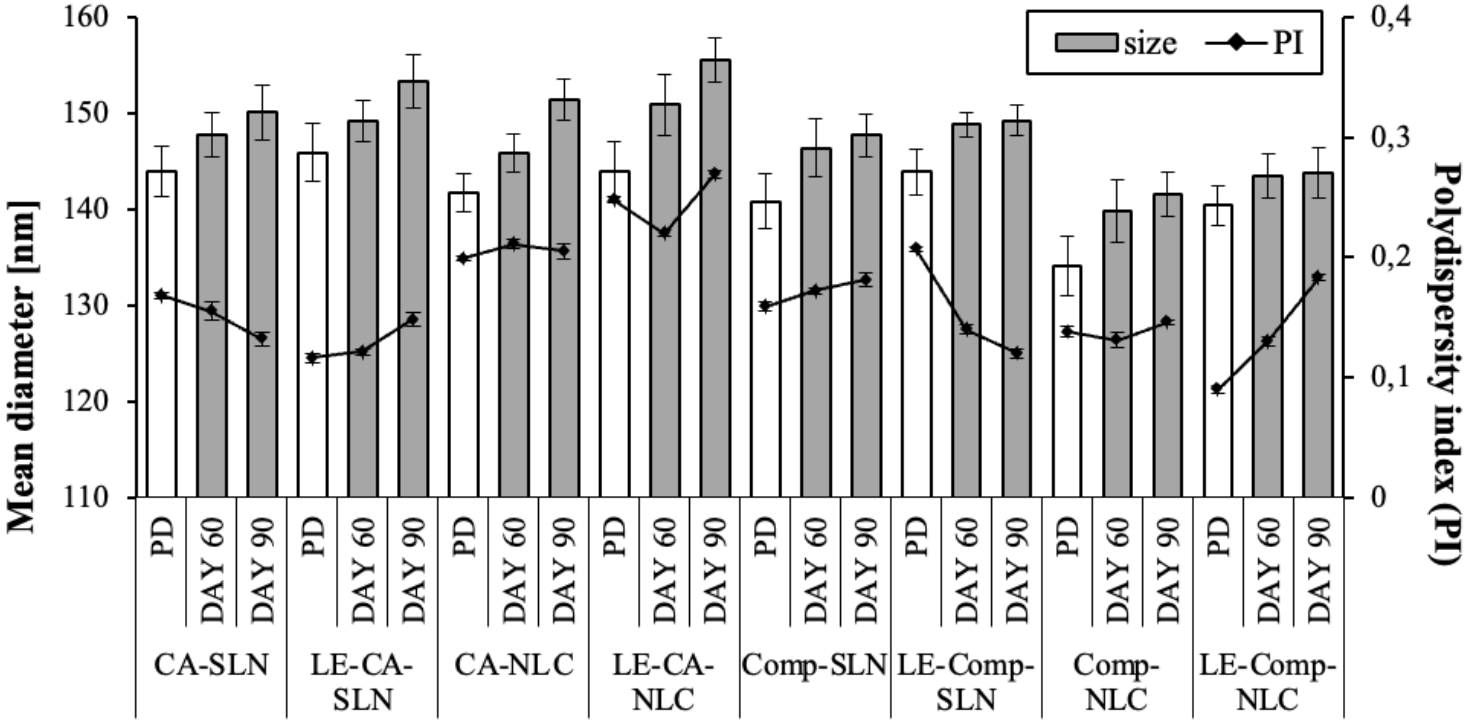

Figure 3

Particle size (nm) and polydispersity index (PI) of formulations for 3 months (PD: production day).

Figure 4

SEM images of SLN and NLC formulations: (A) CA-NLC, (B) CA-SLN, (C) Comp-NLC, (D) Comp-SLN, (E)LE-CA-NLC, (F)LE-CA-SLN, (G)LE-Comp-NLC and (H) LE-Comp-SLN

Figure 5

EE values of formulations for 3 months (PD: production day).

Figure 6

FT-IR spectrum of pure LE and formulations: (A)Pure drug (LE), (B) Comp-SLN, (C) Comp-NLC, (D) LE-Comp-SLN, (E) LE-Comp-NLC, (F) CA-SLN, (G) CA-NLC, (H) LE-CA-SLN, (I) LE-CA-NLC.

Figure 7

DSC profiles of pure lipids and the formulations. A) Pure Compritol® 888 ATO, B) Comp-SLN, C) Comp-NLC, D) LE-Comp-SLN, E) LE-Comp-NLC, F) Pure Cetyl stearyl Alcohol (CA), G) CA-SLN, H) CA-NLC, I) LE-CA-SLN, J) LE-CA-NLC.

Figure 8

In vitro release profiles of formulations. (Points indicates average value ± SD (n = 6)).

Figure 9

LE permeation through skin of porcine. (Points indicates average value ± SD (n = 6)).

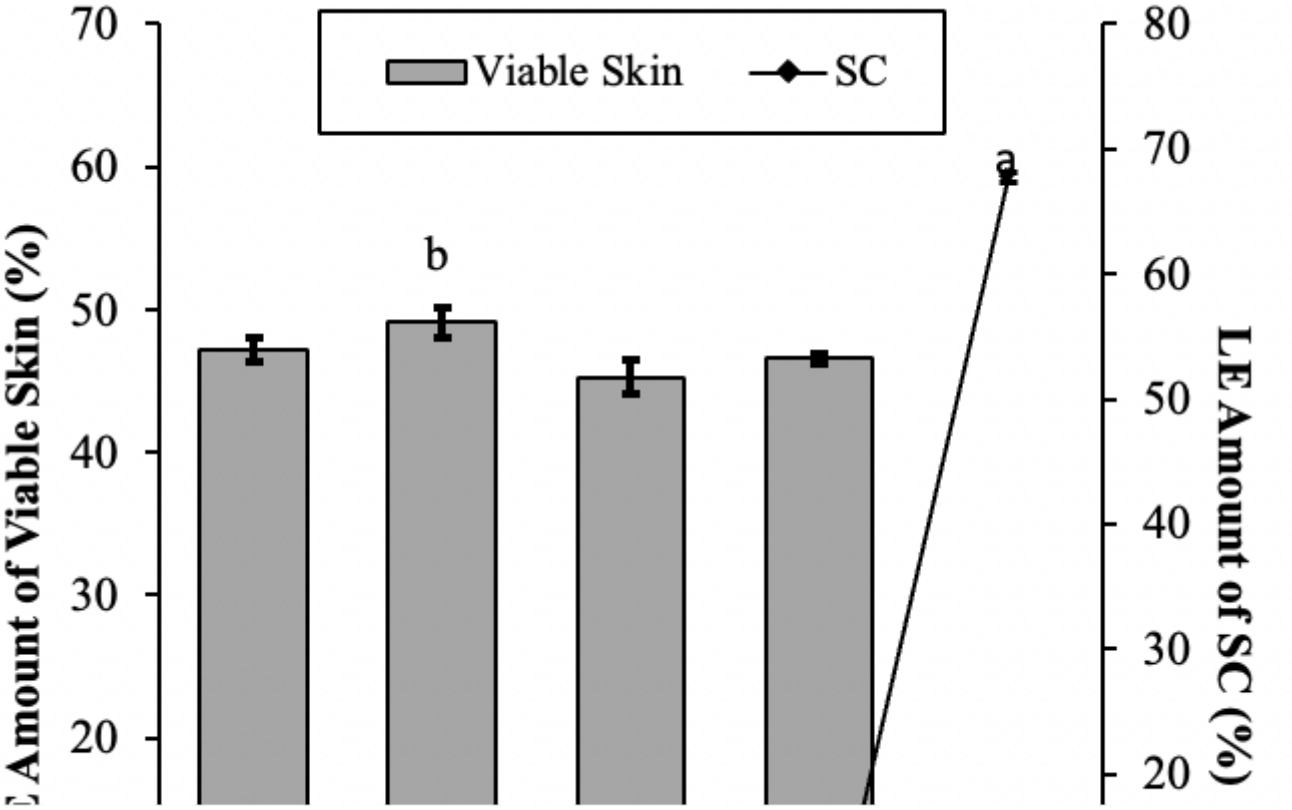

Figure 10

Penetration of LE in the layers of the skin after 8 hours. (a: indicates a statistically significant difference in % of LE between control and other formulations in SC, $p \leq 0.05$, b: indicates a statistically significant difference in % of LE in viable skin layers, $p \leq 0.05$)